**Advances**
2023; 4(1): 36-43
http://www.sciencepublishinggroup.com/j/advances
doi: 10.11648/j.advances.20230401.15

# Finite Deformations of Internally Pressurized Synthetic Compressible Cylindrical Rubber-Like Material

**Egbuhuzor Udechukwu Peter, Udoh Ndipmong Augustine**

Mathematics and Statistics Department, Faculty of Science, Federal University, Otuoke, Nigeria

**Email address:**
egbuhuzorup@fuotuoke.edu.ng (Egbuhuzor Udechukwu Peter), udohna@fuotuoke.edu.ng (Udoh Ndipmong Augustine)

**To cite this article:**
Egbuhuzor Udechukwu Peter, Udoh Ndipmong Augustine. Finite Deformations of Internally Pressurized Synthetic Compressible Cylindrical Rubber-Like Material. *Advances*. Vol. 4, No. 1, 2023, pp. 36-43. doi: 10.11648/j.advances.20230401.15

**Received**: January 27, 2023; **Accepted**: February 24, 2023; **Published**: March 15, 2023

**Abstract:** The finite deformation of internally pressurized isotropic compressible synthetic rubber-like material governed by Levinson and Burgess strain energy function is analysed. A second-order nonlinear ordinary differential (Lane-Emden) equationwith shooting boundary value was derivedfor the determination of displacements distributions. Several analytical methods were employed to solve the resulting boundary value problem but no closed form solution was obtained at the moment. Fortunately, a lot of software have been developed to handle such highly nonlinear second order ordinary differential equations with specific values of parameters. Also, the stresses acting on the material were determined. We obtained numerical solution by applying shooting method and validated the result using collocation method on mathematica (ode45 solver). The simulation of the system is made for$\rho = 14N/m^2$, and the cylindrical symmetric deformation attained its maximum displacements and stresses at$r(1) = 1.16638m$ and $\sigma_{rr}$ = (-1.2973*e*-05)kg/m/s$^2$. We were able to develop numerical schemes using shooting and Collocation methods which made it easier to determine position of maximum stresses and pressure in a cylindrical material of Levinson-Burgess strain energy function. These numerical schemes can solve any nonlinear second-order ordinary differential equations with any given boundary conditions on Mathematica Software. The results of the two schemes were statistically compared using t-test and results obtained showed, the two methods have no significant difference which validates the solutions.

**Keywords:** Deformation, Displacement and Stresses, Levinson and Burgess, Hollow Sphere, Hollow Cylinder

## 1. Introduction

The complexity of mathematical models in the theory of elasticity, particularly in structural modeling, often results is highly challenging and sometimes impossible differential equations, making it difficult to drive analytical or closed form solutions to the problem.

The article "Displacements and Finite-Strain Fields in Hollow Sphere Subjected to Large Elastic Deformations" by Chen and Durelli investigates the finite-strain fields and displacements of a hollow sphere under large elastic deformations [1].

The authors used the theory of finite elasticity and the principle of virtual work to derive the equations governing the displacement and strain fields of the hollow sphere. They consider the case of a thick-walled hollow sphere subjected to an internal pressure and investigate the effect of the Poisson's ratio on the deformation behavior.

The results of the analysis show that the displacement and strain fields are non-uniform and vary significantly across the thickness of the sphere. The authors also demonstrate that the Poisson's ratio has a significant effect on the deformation behavior of the sphere, particularly on the radial and circumferential strains.

The article provides a detailed analysis of the deformation behavior of a hollow sphere under large elastic deformations and highlights the importance of considering the effect of the Poisson's ratio on the deformation behavior. The results of this study can be useful in the design and analysis of structures subjected to large elastic deformations.

This is also related to the work by Huang [2] where the y investigated the problem of finite displacement of a hollow sphere under internal and external pressures.

They derived the governing equations for the finite displacement problem of a thick-walled hollow sphere using the theory of finite elasticity. The equations were solved using the boundary value. The paper Stange discussed the behaviour

of a hollow sphere made of a linear elastic perfectly plastic material under finite deformation [3]. The study uses the theory of large deformations and discusses the equations that govern the deformation of such a material. The author derives the stress-strain relationship and the deformation equations for this type of material and discusses the effects of different parameters on the behavior of the hollow sphere.

The paper also includes numerical examples and a discussion of the results. The author concludes that the behavior of the hollow sphere is highly dependent on the parameters used and that there are many factors that can affect the deformation of such a material. The study provides valuable insights into the behavior of linear elastic perfectly plastic materials under finite deformation and has applications in various engineering fields.

Overall, the article is a valuable contribution to the field of mechanics and provides important insights into the behavior of linear elastic perfectly plastic materials under large deformations. Hill discussed the problem of cylindrical and spherical inflation in the context of compressible finite elasticity, and presents a mathematical model for analyzing the problem [4]. The article also provides numerical solutions to the model, and discusses the physical implications of the results.

In this paper, we have extended the work done by Egbuhuzor and Erumaka where they considered the finite deformation of internally pressurized spherical rubber-like materials [6] by considering the paper written by Levinson and Burgess. They discussed the behavior of rubber-like materials that are only slightly compressible. The authors compared different constitutive models that can be used to describe the material behavior, including the Mooney-Rivlin model, the Ogden model, and the neo-Hookean model.

The Mooney-Rivlin model is a two-term polynomial model that can be used to describe the stress-strain relationship of rubber-like materials. The Ogden model is a more complex model that uses multiple terms to describe the material behavior. The neo-Hookean model is a simpler model that assumes the material is incompressible.

The authors compared these models using experimental data from a uniaxial tension test on a rubber sample. They find that the Mooney-Rivlin and Ogden models provide better fits to the experimental data than the neo-Hookean model. However, they also note that the more complex Ogden model may not be necessary for describing the behavior of slightly compressible rubber-like materials [5].

Overall, the article provides valuable insights into the behavior of rubber-like materials and the different constitutive models that can be used to describe their behavior. Egbuhuzor and Erumaka modelled the Levinson and Burgess strain energy function where they derived a second order nonlinear ordinary differential equations through which they determined the stresses and displacement distributions of the material. Their work is an offshoot ofthe work by Levinson and Burgess who were able to obtain the different behaviours of the polynomial materials and compared it with different other strain energy functions. Rubber is not just about the original natural rubber but also referred to any material that has similar mechanical properties and they are in other words said to be rubber-like materials.

Aani and Rahimi determined the stresses and displacements of axisymmetric radial deformation of the shell. They applied Neo-Hookean strain energy function to obtain the behaviour of the material. Results show that the outer and inner radius is an important parameter which can be mirrored to some applications in order to control the stresses [7]. In another paper, they also used Donnell nonlinear theory to derive the equilibrium equations of the shells, and the Rayleigh-Ritz method to obtain the critical buckling loads for both spherical and cylindrical shells. They considered different boundary conditions and material property distributions, and analyze the effects of these parameters on the shell's stability. The paper provides a deatailed analysis of the stability of functionally graded thick-walled shells under internal pressure, which is an important topic in the design and analysis of pressure vessels and pipelines. The results can be used to optimize the design of these structures to ensure the safe operation under different loading conditions [8].

On Simple shear of a compressible quasilinear viscoelastic material as presented by De Pascalis. They explained the effects of compressibility on the subsequent deformation and stress fields that result to isochoric deformation, and calculations of the dissipated energy associated with both a ramp simple shear profile and oscillatory shear are given [9]. To illustrate their results, choosing the compressible Neo-Hookean model proposed by Levinson and Burgess and from their results, the rates of deformation were discovered to be slow enough that inertia effects can be neglected. Guiseppe P. and Giuseppe S reviewed important areas of Gent constitutive model for rubberlike materials.

Their research was based on damageable materials where they explained certain damage and deformation localization. They observed that Gent behaves as the neo-Hookean model at low strain. The clear and simple mathematical structure of the Gent model allows one to use generalized constitutive theories beyond classical Taylor expansions [10].

Blatz and Ko proposed a strain energy function which they called "Standard" strain energy function but Levinson and Burgess in their work discovered that there were certain limitations. First, in the limit of incompressibility, the standard strain energy function cannot represent Mooney-Rivlin or Neo-Hookean material and secondly, It is not a capable strain energy function for an isotropic material [11].

Chung et al in their work on the finite deformation of internally pressurized hollow cylinders and spheres for a class of compressible elastic materials considered hollow circular cylinders and spheres deorming under applied internal pressure condition for the initiation of localized shear bifurcation. It is shown that when the ratio of the outer undeformed radius to the inner undeformed radius is larger than the critical value, the shear bifurcation occurs before the maximum pressure is reached, while when the ratio is smaller than the critical value, the converse is true. This analysis was carried out for a particular compressible elastic foam rubber

material (Blatz-Ko) [12]. This strain energy function was derived from the work of Chung et al. They derived a boundary value model equatrion using condition for foam rubber. The resulting second order ordinary differential equations are solved in closed form for the determination of the displacement distributions.

Horgan worked on remarks on ellipticity for the generalized Blatz-Ko constitutive model for a compressible nonlinearly elastic solid. They presented an expression for strain energy density per unit undeformed volume for homogeneous isotropic elastic compressible material [13].

Levinson and Burgess were primarily concerned with the strain energy function of a highly compressible polyurethane foam rubber for which they found experimentally that $f = 0$ and $v = 0.25$ but for a solid rubber of the same chemical composition, it was found that $f = 1$ and $v = 0.46$. Since for the incompressible case the I and J invariants become identical, compressible generalizations of the neo-Hookean and Mooney-Rivlin material clearly may be made in terms of either set of invariants.

The strain energy density for a compressible hyperelastic material which reduces to the Mooney-Rivlin material as v tends to 0.5 was also obtained by Horgan.

Kulcu examined a new strain energy function to describe the hyperelastic behaviour of rubber-like materials under various deformation. The proposed strain energy function represents an invariant based model which has two material constants. This model was tested with the experimental data of vulcanized rubbers, collagen and fibrin just like Levinson and Burgess did [14]. The parameters were kept constant when placed under certain types of loads. There was an agreement between the model and the experimental data for all materials.

Akhundov and Lunev improved on their earlier work by solving the problem of tyre. The model made use of applied theory of vibrous material with small and large strains. They determined the strain, stresses and displacement distribution undergone by the tyre under pressure [15].

Some other authors introduced many other approach to solving the problems of hyperelastic models. Fereidoonnezhad instead of applying failure, rather used their proposed strain energy function to characterize the behaviour of a tranversely isotropic incompressible fibre reinforced rubber. The result of their prediction agreed with the experimental data for both tensile and shear deformations [16]. Moreira and Numes compared two types of deformation using experimental and theoritical methods. Result showed that simple shear cannot be considered as pure shear combined with a rotation when undergoing large deformation. It is a fact that rubber-like materials undergo large deformation and nonlinearly upon loading and they return to the initial configuration after the removal of load [17]. Pence and Gou considered three different compressible versions of the conventional incompressible neo-Hookean material model. The three versions critically considered the differences with respect to each other by use of neo-Hookean strain energy function. They exhibited these differences which their work effectively addressed.

The difference between these literatures and our work is the fact that none to our knowledge has investigated the usefulness of the strain energy function of Levinson and Burgess in determining the displacements and stresses of deformations involving both the spherical and cylindrical coordinate systems. Levinson and Burgess compared other strain energy functions using the poisson ratio and material constant to determine the behaviour of the materials [18].

This work is another dimension to the work of Levinson and Burgess. We considered the problem as a hollow sphere and hollow cylinder similar to the work of Blatz and Ko. The difference beetween our work and Blatz and Ko is that they considered the strain energy function of foam rubber ($f = 0$ and $v = 0.25$). Similarly, Levinson and Burgess in their work also focused only on highly compressible foam rubber. In this work, we considered the strain energy function when $f = 1$ and $v = 0.46$ which is said to be a solid (synthetic) rubber as shown in the paper by Egbuhuzor and Erumaka. We also derived the second order nonlinear ordinary differential equations with appropriate boundary value conditions which were simulated using mathematica software for the determination of stresses and displacements.

# 2. Methodology

### *2.1. Field Equation for Symmetric Deformation of a Cylindrical Material of Levinson-Burgess*

We consider the case of deformation that takes the point $(R, \Theta, Z)$ of the cylinder in the undeformed configuration to $(r, \theta, z)$ in the deformed configuration such thatthis represents a three dimensional cross-section of a solid cylinder with an internal and external radii a and b in its undeformed form as proposed in Chung et al.

$$r = r(R) \qquad a \leqslant R \leqslant b$$

$$\theta = \Theta \qquad 0 \leqslant \Theta \leqslant 2\pi$$

$$z = \gamma Z \qquad 0 \leqslant Z \leqslant l$$

$$\frac{dr}{dR} > 0$$

where $\gamma$ is a material constant

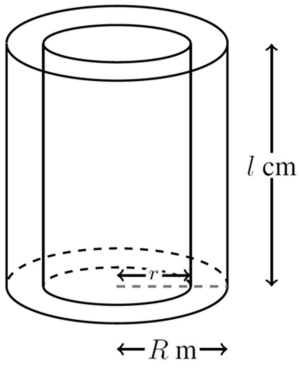


***Figure 1.*** *Hollow Cylindrical shape.*

For this case, the deformation gradient tensor $\bar{F}$ and Cauchy Green Right tensor (C) are given by;

$$\bar{F} = \begin{matrix} (\frac{dr}{dR}) & 0 & 0 \\ 0 & (\frac{r}{R}) & 0 \\ 0 & 0 & (\gamma) \end{matrix} \quad (1)$$

$$\bar{C} = \bar{F}^T \bar{F} = \begin{matrix} (\frac{dr}{dR})^2 & 0 & 0 \\ 0 & (\frac{r}{R})^2 & 0 \\ 0 & 0 & (\gamma)^2 \end{matrix} \quad (2)$$

The principal invariants are:

$$I_1 = tr\bar{C} = (\frac{dr}{dR})^2 + (\frac{r}{R}) + (\gamma)^2, \quad (3)$$

$$I_2 = \frac{1}{2}[(tr\bar{C})^2 \quad tr(\bar{C})^2] = (\frac{r}{R})^2(\frac{dr}{dR})^2 + (\frac{r^2\gamma^2}{R^2}) + (\gamma)^2(\frac{dr}{dR})^2 \quad (4)$$

$$I_2 = \frac{1}{2}[(tr\bar{C})^2 \quad tr(\bar{C})^2] = (\frac{r}{R})^2(\frac{dr}{dR})^2 + (\frac{r^2\gamma^2}{R^2}) + (\gamma)^2(\frac{dr}{dR})^2 \quad (5)$$

Using Cauchy tensor as defined below;

$$\sigma_{ii} = \frac{\lambda_i}{\lambda_1\lambda_2\lambda_3}\frac{\partial W}{\partial \lambda_i}, \text{ for i = 1,2,3} \quad (6)$$

We obtain;

$$\sigma_{11} = \sigma_{rr} = \frac{\mu_0}{2}[\frac{2r'}{r\gamma}R + \frac{25r'\gamma}{R}r \quad 27] \quad (7)$$

$$\sigma_{22} = \sigma_{\theta\theta} = \frac{\mu_0}{2}[\frac{2r}{r'R\gamma} + \frac{25r'r\gamma}{R} \quad 27] \quad (8)$$

$$\sigma_{33} = \sigma_{zz} = \frac{\mu_0}{2}[\frac{2R\gamma}{r'r} + \frac{25r'r\gamma}{R} \quad 27] \quad (9)$$

where $\sigma_{r\theta} = \sigma_{\theta r} = \sigma_{\theta z} = \sigma_{z\theta} = \sigma_{rz} = \sigma_{zr} = 0$

According to [12], the equilibrium equation after applying the cauchy stresses above is given as;

$$\frac{d\sigma_{rr}}{dR} + \frac{r'}{r}[\sigma_{rr} \quad \sigma_{\theta\theta}] = 0, \quad (10)$$

Applying (7) and (8) in (10), we obtain the nonlinear ordinary differential equation as;

$$(2R^3 + 25r^2R\gamma^2)\frac{d^2r}{dR^2} + 25r\gamma^2R(\frac{dr}{dR})^2 \quad (2R^2 \quad 25r^2\gamma^2)\frac{dr}{dR} \quad 2rR = 0 \quad (11)$$

### *2.2. Shooting Boundary Conditions*

$$(\sigma_{rr})_{R=a} = \rho \quad as;$$

$$r'(a) = \frac{r(a)\gamma(27 \quad \frac{2\rho}{\mu})}{2a^2 + 25r^2(a)\gamma^2} \quad (12)$$

$$(\sigma_{rr})_{R=b} = 0$$

$$r'(b) = \frac{27br(b)\gamma}{2b^2 + 25r^2(b)\gamma^2} \quad (13)$$

# 3. Results and Discussion Solutions for Cylindrical Symmetric Deformation

At this point, we determined the displacements and stresses of the compressible cylindrical rubber-like material undergoing internal pressure. First, we consider the derived equation of cylindrical symmetric deformations which we solved numerically usingshooting and collocation methods on Mathematica (ode45 solver). The boundary value problem is a Lame-Emden second-order nonlinear ordinary differential equations and at the moment, no closed form solution has been found for this model equation with shooting boundary conditions. The load applied is the same at every height and the load considered here is the pressure which is applied at a constant rate at the inner surface as seen in the spherical deformation reported by Egbuhuzor and Erumaka. This load generates stresses within the cylinder and the outer surface is stress free.

### *3.1. Collocation Method for Nonlinear Second-Order Boundary Value Problems*

The paper by [6] first stated the Exponentially fitted backward differentiation scheme for general second order differential equations derived using collocation method, with frequency $w = 1$, $\gamma = 1.0315$, $h = \frac{(b \quad a)}{N}$; where (a,b) is the interval of integration, N is number of subintervals and $a = x_0 < x_1 < .... < x_N = b$.

$$y_{2+i} = \frac{1}{((-1+e^{hw})^2 w^2)}(f_i - 2e^{hw}f_i + e^{2hw}f_i - e^{hw}h^2w^2f_i - 2f_{1+i} + 4e^{hw}f_{1+i} - 2e^{2hw}f_{1+i} + h^2w^2f_{1+i} + e^{2hw}h^2w^2f_{1+i} + f_{2+i} - 2e^{hw}f_{2+i} + e^{2hw}f_{2+i} - e^{hw}h^2w^2f_{2+i} - w^2y_i + 2e^{hw}w^2y_i - e^{2hw}w^2y_i + 2w^2y_{1+i} - 4e^{hw}w^2y_{1+i} + 2e^{2hw}w^2y_{1+i})$$

$$yp_i = \frac{-1}{6(-1+e^{hw})^2hw^2}(-6f_i] + 6e^{hw}f_i - 6f_i - 5e^{hw}h^2w^2f_i + 2^{2hw}h^2w^2f_i + 12f_{1+i} - 12e^{hw}f_{1+i} + 12hwf_{1+i} + 5h^2w^2f_{1+i]} + e^{2hw}h^2w^2f_{1+i} - 6f_{2+i} + 6e^{hw}f_{2+i} - 6hwf_{2+i} - 2h^2w^2f_{2+i} - e^{hw}h^2w^2f_{2+i} + 6w^2y_i - 12e^{hw}w^2y_i + 6e^{2hw}w^2y_i - 6w^2y_{1+i} + 12e^{hw}w^2y_{1+i} - 6e^{2hw}w^2y_{1+i})$$

$$yp_{1+i} = \frac{1}{6(-1+e^{hw})^2hw^2}(6f_i - 6e^{hw}f_i + 6e^{hw}hwf_i - 4e^{hw}h^2w^2f_i + e^{2hw}h^2w^2f_i - 12f_{1+i} + 12ehwf_{1+i} - 12e^{hw}hwf_{1+i} + 4h^2w^2f_{1+i} + 2e^{2hw}h^2w^2f_{1+i} + 6f_{2+i} - 6e^{hw}f_{2+i} + 6e^{hw}hwf_{2+i} - h^2w^2f_{2+i} - 2e^{hw}h^2w^2f_{2+i} - 6w^2y_i + 12e^{hw}w^2y_i - 6e^2hww^2y_i + 6w^2y_{1+i} - 12e^{hw}w^2y_{1+i} + 6e^{2hw}w^2y_{1+i})$$

$$yp_{2+i} = \frac{-1}{6(-1+e^{hw})^2hw^2}(-6f_i + 6e^{hw}f_i - 6e^{2hw}hwf_i + 7e^{hw}h^2w^2f_i + 2e^{2hw}h^2w^2f_i + 12f_{1+i} - 12e^{hw}f_{1+i} + 12e^{2hw}hwf_{1+i} - 7h^2w^2f_{1+i} - 11e^{2hw}h^2w^2f_{1+i} - 6f_{2+i} + 6E^{hw}f_{2+i} - 6e^{2hw}hwf_{2+i} - 2h^2w^2f_{2+i} + 11e^{hw}h^2w^2f_{2+i} + 6w^2y_i - 12e^{hw}w^2y_i + 6e^{2hw}w^2y_i - 6w^2y_{1+i} + 12e^{hw}w^2y_{1+i} - 6e^{2hw}w^2y_{1+i}$$

### *3.2. Results and Discussions*

***Table 1.*** *Table for cylindrical shooting method Versus Collocation method from (11) at N= 40.*

| R | R (R) (shooting method) | R (R) Derived method | $\sigma_{rr}$ (shooting/derived method) |
|---|---|---|---|
| 0.20 | 0.39735 | 0.39731 | 8.7399/8.7384 |
| 0.22 | 0.42188 | 0.42184 | 7.8131/7.8118 |
| 0.24 | 0.44572 | 0.44567 | 7.0302/7.0288 |
| 0.26 | 0.46896 | 0.46891 | 6.3595/6.3583 |
| 0.28 | 0.49167 | 0.49162 | 6.9852/9839 |
| 0.30 | 0.51392 | 0.51387 | 5.2697/5.2686 |
| 0.32 | 0.53575 | 0.53570 | 4.8205/4.8196 |
| 0.34 | 0.5572 | 0.55715 | 4.4209/4.4200 |
| 0.36 | 0.57832 | 0.57826 | 4.0632/4.0622 |
| 0.38 | 0.59912 | 0.59907 | 3.7406/3.7398 |
| 0.40 | 0.61964 | 0.61958 | 3.4486/3.4477 |
| 0.42 | 0.63990 | 0.63984 | 3.1827/3.1819 |
| 0.44 | 0.65992 | 0.65986 | 2.9398/2.9391 |
| 0.46 | 0.67972 | 0.67965 | 2.7170/2.7161 |
| 0.48 | 0.69932 | 0.69925 | 2.5117/2.5109 |
| 0.50 | 0.71872 | 0.71865 | 2.3220/2.3212 |
| 0.52 | 0.73794 | 0.73787 | 2.1463/2.1455 |
| 0.54 | 0.75700 | 0.75693 | 1.9829/1.9822 |
| 0.56 | 0.77591 | 0.77583 | 1.8309/1.8302 |
| 0.58 | 0.79467 | 0.79459 | 1.6889/1.6882 |
| 0.60 | 0.81330 | 0.81321 | 1.5562/1.5553 |
| 0.62 | 0.83179 | 0.83171 | 1.4314/1.4307 |
| 0.64 | 0.85017 | 0.85009 | 1.3144/1.3137 |
| 0.66 | 0.86843 | 0.86835 | 1.1620/1.1613 |

| R | R (R) (shooting method) | R (R) Derived method | $\sigma_{rr}$ (shooting/derived method) |
|---|---|---|---|
| 0.68 | 0.88659 | 0.88650 | 1.1004/1.0097 |
| 0.70 | 0.90465 | 0.90456 | 1.0023/1.0016 |
| 0.72 | 0.92261 | 0.92252 | 0.9096/0.9089 |
| 0.74 | 0.94048 | 0.94039 | 0.8218/0.8212 |
| 0.76 | 0.95827 | 0.95817 | 0.7387/0.7380 |
| 0.78 | 0.97597 | 0.97587 | 0.6596/0.6590 |
| 0.80 | 0.99360 | 0.99350 | 0.5846/0.5840 |
| 0.82 | 1.01115 | 1.01105 | 0.4871/0.4866 |
| 0.84 | 1.02864 | 1.02853 | 0.4452/0.4445 |
| 0.86 | 1.04605 | 1.04595 | 0.3803/0.3797 |
| 0.88 | 1.06341 | 1.06330 | 0.3184/0.3178 |
| 0.90 | 1.08070 | 1.08060 | 0.2593/0.2588 |
| 0.92 | 1.09794 | 1.09783 | 0.2029/0.2023 |
| 0.94 | 1.11513 | 1.11502 | 0.1488/0.1482 |
| 0.96 | 1.13226 | 1.13215 | 0.0971/0.0965 |
| 0.98 | 1.14934 | 1.14923 | 0.0475/0.0470 |
| 1.00 | 1.16638 | 1.166263 | -1.2973e-05/-5.8495e-04 |

Graphical representation of the solution

```
Plot[Evaluate[r[R] /. sols], {R, 0.2, 1}, PlotStyle → {Thick}]
```

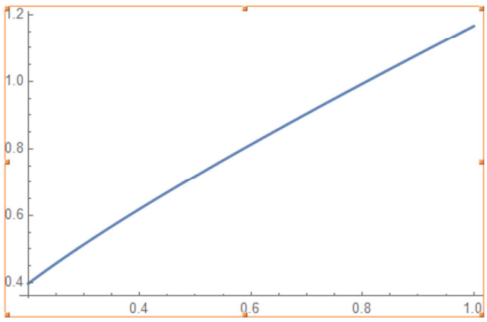


***Figure 2.*** *Cylindrically symmetric deformation for N = 40.*

For $N = 40$, the graph above describes the cylindrical deformation of the nonlinear ODE of equation (11) using shooting method on Mathematica at $r(0.2) = 0.39735m$ and $r(1) = 1.16638m$ when maximum $\rho = 14N/m^2$. There is steady increase in displacements when the pressure increases. The material will blow up when it exceeds the maximum pressure. This is true for figure 3 which shows the graph of the two methods for validation of our results Figure 2 is simply the number of iterations which is N = 40.

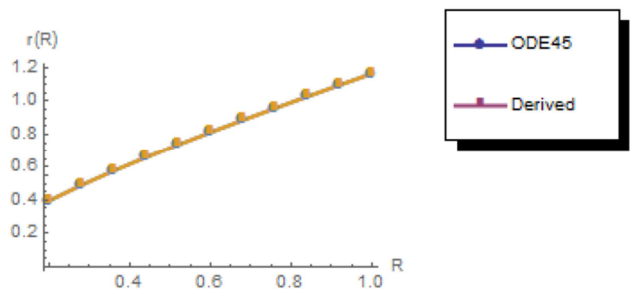


***Figure 3.*** *Cylindrical (shooting method) and Collocation method for N = 40.*

Figure 4 is the plot of the gradient against the radius R. The $r'(R)$ helped us to obtain the stresses acting on the material. At $R = 0.2m$, the gradient $r'(R) = 1.24m$ for the cylindrical deformation which serves as their point of interception. This shows changes on the materials as regards the stresses. Figure 4 shows that $r'(R)$ is decreasing and both are said to be concave down. They are also less steep. Figure 4 has a horizontal asymptote at $R = (0.2,1)$. Note that the radius of a circle, a sphere or cylinder and any other shape with circular surface on it is a measurement. For us to have obtained a negative radius, it shows that there is more than one center and at this point, the circumference becomes the center.

Graphical representation of the solution

```
Plot[Evaluate[r'[R] /. sols], {R, 0.2, 1},
 AxesLabel → {"R", "r'(R)"}]
```

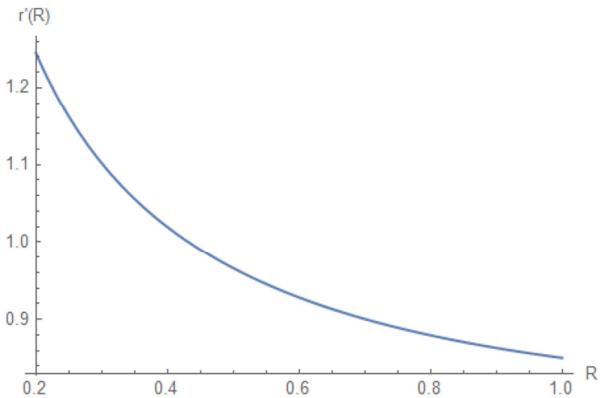


***Figure 4.*** *Graph for r'(R) Versus R.*

## 4. Analysis of Results

The displacements for the cylindrical deformation at $r(a)$ and $r(b)$ are $r(0.2) = 0.39735m$ and $r(1) = 1.16638m$ and corressponding stresses of $\sigma(r(0.2)) = 8.7399kg/m/s^2$

and $\sigma(r(1)) = 1.2973e\ \ 05kg/m/s^2$ for the shooting method and for the collocation method we obtained $r(0.2) = 0.39731m$ and $r(1) = 1.16626m$ with stresses $\sigma(r(0.2)) = 8.7384kg/m/s^2$ and $\sigma(r(1)) = 5.849e\ \ 04kg/m/s^2$ respectively. It is found that as the pressure increases, the stress acting on the material also increases. There are significant variations in the stresses and even at different points of radius.

If the pressure increases beyond that, the material inflates, reaches a amximum with value $r(1) = 1.16626m$. The table compares the solution as obtained using shooting method internally in mathematica (ode45 solver) and the derived collocation method applied to obtain the results for displacements.

It is well known that the displacement equations of equilibrium in finite elastostatics may lose ellipticity at sufficiently large deformations. The existence of smooth solution is obtained after loss ellipticity. Moreover, the possibilty exists that non-smooth deformation fields with discontinuous deformation gradients and stresses might occur. This can be compared with the arguement shown in Chung et al where they deduced that as the pressure, $\rho$, is increased, the deformed radius increases until $\rho$ reaches a maximum value where r(1) = 0.03705. Our results are in agreement with this work by Chung et al who also showed that axisymmetric solutions with discontinuities do not exist in their work. If Weak solution exists, then it must be non-axisymmetric.

# 5. Conclusion and Recommendation

### *5.1. Conclsuion*

We used the results obtained to calculate stresses and displacements in radial deformation. This was achieved numerically at maximum pressures using the Mathematica algorithm (ode45 solver), which internally employed the shooting method. We validated the shooting method with the collocation method. The argument posed by [12] is that as the pressure ( $\rho$ ) increases, the deformed radius increases until $\rho$ reaches its maximum value where $r(a) = 1$.

In our work, axisymetric solutions with discontinuities do not exist. If weak solution exist, they must be axisymmetric. As the pressure increases, the material inflates. Our results show that the cylindrical symmetric deformation attains its maximum pressure at $\rho = 14N/m^2$ and when for example, the material is inflated too much, the rubber rounds out at the top of the material and it will quickly wear out. There will be traction reduction which is responsible for the material to burst. This research work can be applied to the problem of radial tyre under internal pressure.

### *5.2. Contribution*

1) In our work, we were able to determine the general equation for the pressure ( $\rho$ ) in a general material composed of Levinson-Burgess strain energy function, which hitherto had been avoided by other authors.
2) We were able to develop numerical schemes using shooting and Collocation methods which makes it easy to determine position of maximum stresses and pressure in a cylindrical material of Levinson-Burgess strain energy function. These numerical schemes can solve any nonlinear second-order ordinary differential equations with any given boundary conditions on Mathematica Software.

### *5.3. Recommendation*

1) We recommend that the strain energy function of Levinson and Burgess be compared with the strain energy functions of other rubber-like materials such as Neo-Hookean, Mooney-Rivlin and other using the same boundary conditions for the determination of the behaviour of the materials.
2) Finite element method can be applied on Matlab for an improved result especially when considering the displacement distribution and stresses acting on a tyre when in contact with the soil under internal pressure.
3) Since we have not been able to get the analytical solution, closed form solution of the nonlinear second-order ordinary differential equations obtained by analytical methods will make a huge contribution to knowledge.

# References

[1] Chen, T. L. and A. J. Durelli, Displacements and Finite-Strain Fields in Hollow Sphere Subjected to Large Elastic Deformations. International Journal of Mechanical Sciences, 1974. 16: p. 777-788.

[2] Huang, Z., On the Finite Displacement Problem of a Hollow Sphere Under Internal and External Pressures. Applied Mathematics and Mechanics, 6, 1097-1102.

[3] Stange, J. B., Finite Deformation of Hollow Sphere of Linear Elastic Perfectly Plastic Material. Acta Mechanica, 1984, 50: p. 201-209.

[4] Hill, J. M., Cylindrical and Spherical Inflation in Compressible Finite Elasticity. IMA Journal of Applied Mathematics, 1992. 50: p. 195-201.

[5] Levinson, M. and I. W. Burgess, A Comparison of some simple constitutive relations for slightly compressible rubber-like materials. International Journal of Mechanical Sciences, 1971. 13: p. 563-572.

[6] Egbuhuzor, U. P, and E. N. Erumaka, Finite Deformation of Internally Pressurized Spherical Compressible Rubber-like Material. Asian Research Journal of Mathematics, 16 (3), 2020. 16 (3): p. 38-49.

[7] Aani, Y. and G. H. Rahimi, On the stability of internally pressurized thick-walled spherical and cylindrical shells made of functionally graded incompressible hyperelastic material. Latin American Journal of Solids and Structures, 2018. 15 (4).

[8] Aani, Y. and G. H. Rahimi, Stress analysis of thick pressure vessel composed of incompressible hyperelastic materials, International Journal of Recent Advances in Mechanical Engineering, 2015. 4 (3): 19-37.

[9] De Pascalis, R., I. D., Abrahams and W. J. Parnell, Simple shear of a compressible quasilinear viscoelastic material. International Journal of Engineering Science, 2015, 88: p. 64-72.

[10] Giuseppe, P. and S. Giuseppe, The Gent model for rubber-like materials: An appraisal for an ingeniousand simple idea. International Journal of Non-Linear Mechanics, 2015, 68: p. 17-24.

[11] Blatz, P. J. and W. L. Ko, Constitutive model in nonlinear finite element analysis. Trans. Soc. Rheol., 1962, 6: p. 223 - 251.

[12] Chung, D. T., C. O. Horgan and R., Abeyaratne, The finite deformation of internally pressurized hollow cylinders and spheres for a class of compressible elastic materials. International Journal of Solids and Structures, 1986, 22 (12): p. 1557-1570.

[13] Horgan, C. O., Remarks on ellipticity for the generalized Blatz-Ko constitutive model for compressible nonlinearly elastic solid. Journal of Elasticity, 1986, 42: 165-176.

[14] Kulcu, I. D., A hyperelastic constitutive model for rubber-like materials. *Archive of Applied Mechanics*, 2019, 1-8.

[15] Akhundov, V. M. and Lunev, V. P. (2013). Modeling of the forming of radial tyre carcass based on applied theory of fibre-reinforced materials. *International Polymer Science and Technology*, 2013, 40 (10): 37-40.

[16] Fereidoonnezhad, B., Naghdabadi, R. and Arghavani, J., A hyperelastic constitutive model for fibre-reinforced rubber-like materials. *International Journal of Engineering Science*, 2013, 71: 36-44.

[17] Moreira, D. C., and Numes, L. C., Comparison of simple and plane shear for an incompressible isotropic hyperelastic material under large deformation. *Polymer Testing*, 2013, 32 (2): 240-248.

[18] Pence, T. J., and Gou, K., On compressible versions of the incompressible neo-Hookean material. *Mathematics and Mechanics of Solids*, 2015, 20 (2): 157-182.